# Numerical Analysis and Optimization of Divertor Cooling System

Andrei Khodak, Michael A. Jaworski
Princeton Plasma Physics Laboratory, Princeton, New Jersey, USA
akhodak@pppl.gov

***Abstract*—Novel divertor cooling system concept is currently under development at Princeton Plasma Physics Laboratory (PPPL). This concept utilizes supercritical carbon dioxide as a coolant for the liquid lithium filled porous divertor front plate. Coolant is flowing in closed loop in the T tube type channel. Application of $CO_2$ eliminates safety concerns associated with water cooling of liquid lithium systems, and promises higher overall efficiency compared to systems using He as a coolant**

**Numerical analysis of divertor system initial configuration was performed using ANSYS software. Initially conjugated heat transfer problem was solved involving computational fluid dynamics (CFD) simulation of the coolant flow, and heat transfer in the coolant and solid regions of the cooling system. Redlich Kwong real gas model was used for equation of state of supercritical CO2 together with temperature and pressure dependent transport properties. Porous region filled with liquid lithium was modeled as a solid body with liquid lithium properties. Evaporation of liquid lithium from the front face was included via special temperature dependent boundary condition. Results of CFD and heat transfer analysis were used as external conditions for structural analysis of the system components. Simulations were performed within ANSYS Workbench framework using ANSYS CFX for conjugated heat transfer and CFD analysis, and ANSYS Mechanical for structural analysis.**

**Initial results were obtained using simplified 2D model of the cooling system. 2D model allowed direct comparison with previous cooling concepts which use He as a coolant. Optimization of the channel geometry in 2D allowed increase in efficiency of the cooling system by reducing the total pressure drop in the coolant flow. Optimized geometrical parameters were used to create a 3D model of the cooling system which eventually can be implemented and tested experimentally. 3D numerical simulation will be used to validate design variants of the divertor cooling system**

***Keywords—divertor; cooling system; lithium; numerical simulations computational fluid dynamics***

## I. INTRODUCTION

Liquid metal plasma-facing components (LMPFCs) are a potentially attractive technology for future power reactors. Examination of the state-of-the-art in cooling technologies indicates that thin-film LM-PFCs will likely operate at 700-800C – a temperature range where strong evaporation/erosion would be expected from liquid lithium surfaces. This regime of operation may lead to novel divertor configurations where the incident heat flux to the PFC surface is mitigated by continuous vapor-shielding.

This work supported by the US DOE Contract No. DE-AC02-09CH11466.

Whereas conventional PFCs rely on water cooling when active cooling is required, future power reactors will utilize gas cooling for higher thermal efficiency. With the use of liquid lithium, there is a necessity to utilize gas cooling for safety reasons. Gas cooling requires high working pressures to obtain reasonable cooling efficacy and suitable control of front-face temperatures under fusion-relevant heat fluxes.

In an attempt to improve thermal performance of conventional helium cooling, alternative coolants are being considered, notably supercritical $CO_2$ This improvement in cooling capabilities could be critical to implementing liquid lithium PFCs, in particular, to avoid excess evaporation and erosion where possible.

To increase efficiency T-tube configuration is used in the divertor cooling system (fig.1.). T-tube geometry have already indicated advantages (in terms of peak surface temperatures) in reducing the overall dimension of the component. For instance, pipe-wall thickness scales with the diameter for constant stress. However, thinner walls result in lower temperature differences for a given heat-flux.

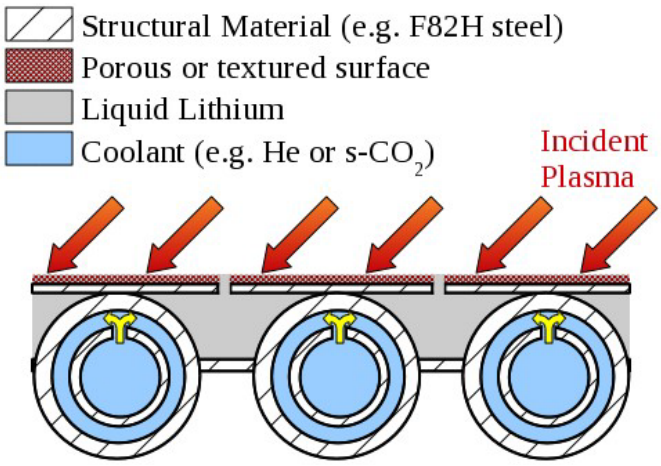


Fig. 1. Schematic of the divertor cooling system using T-tube

## II. NUMERICAL MODEL

### A. General Description

To simulate performance of the cooling system, fluid dynamics, thermal and structural analysis was performed using the numerical model based on the ANSYS software.

Conjugated heat transfer analysis model was created using ANSYS CFX [1]. This model solves discretized Reynolds averaged Navier Stokes equations to resolve flow of coolant.

Simultaneously energy equation is solved to resolve heat transfer in both solid and fluid regions. On the interface between solid and fluid regions non-slip conditions were imposed for the coolant flow using wall functions approach for turbulent flow. Conservation of the heat flux on fluid solid interface was also assumed.

Temperature dependent properties of the materials are used for solid parts. Real gas model with temperature and pressure dependent transport properties are used for supercritical $CO_2$. Ideal gas model with temperature dependent transport properties is used for Helium flow. Heat flux distribution on the font wall includes evaporative heat flux from Lithium surface.

Results of heat transfer simulations were used to impose temperature and pressure loads for structural simulations using ANSYS structural [2]. Interpolation of the of the temperature and pressure fields on the mesh for structural analysis was performed in ANSYS Workbench environment.

*B. Modeling of coolant properties*

Real gas properties of super critical $CO_2$ were modeled using Aunglier Redlich Kwong model available in ANSYS CFX [1] with the following equation of state:

$$p = \frac{R_{CO_2}T}{1/\rho - b + c} - \frac{\rho a}{1/\rho + b} \tag{1}$$

where:

$$a = \frac{0.42747 {R_{CO_2}}^2 T_{cCO_2}^2}{p_{cCO_2}} \left(\frac{T[K]}{T_{cCO_2}}\right)^{-n}$$

$$b = \frac{0.08664 R_{CO_2} T_{cCO_2}}{p_{cCO_2}}$$

$$c = \frac{R_{CO_2} T_{cCO_2}}{p_{cCO_2} + \frac{\rho_{cCO_2} a}{1/\rho_{cCO_2} + b}} + b - \frac{1}{\rho_{cCO_2}}$$

$$n = 04986 + 1.1735\omega_{CO_2} + 0.4754\omega_{CO_2}^2$$

$$R_{CO_2} = \frac{R}{m_{moleCO_2}} = \frac{8.3144621\, J/(mol \cdot K)}{0.04401\ kg/mol}$$

$$T_{cCO_2} = 304.1282\ K$$

$$p_{cCO_2} = 7.3773\ MPa$$

$$\rho_{cCO_2} = 467.6\ kg/m^3$$

$$\omega_{CO_2} = 0.225$$

Comparison of density data from [3] on fig 2 shows that carbon dioxide exhibits real gas behavior in the range of temperatures below 500K.

Transport properties of CO2 were interpolated using data from [4] for the pressure range used in the current analysis. Relations (2) and (3) provide relations for thermal conductivity and viscosity with the values for constants presented in table 1.

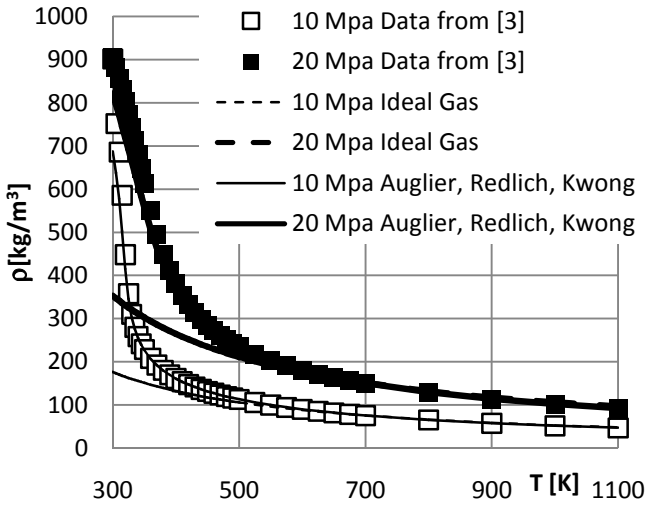


Fig. 2. Density of supercritical $CO_2$

$$\lambda_{CO_2} = \sqrt[4]{\lambda'^4_{CO_2} + \lambda"^4_{CO_2}} \quad mW/(m \cdot K) \tag{2}$$

where:

$$\lambda'_{CO_2} = A'_{\lambda_{CO_2}} + B'_{\lambda_{CO_2}} T[K]$$

$$\lambda"_{CO_2} = A"_{\lambda_{CO_2}} T[K]^{B"_{\lambda CO_2}}$$

$$\mu_{CO_2} = \sqrt[4]{\mu'^4_{CO_2} + \mu"^4_{CO_2}} \quad \mu Pa \cdot s \tag{3}$$

where:

$$\mu'_{CO_2} = A'_{\mu_{CO_2}} + B'_{\mu_{CO_2}} T[K]$$

$$\mu"_{CO_2} = A"_{\mu_{CO_2}} T[K]^{B"_{\lambda CO_2}}$$

TABLE I. COEFFICIENTS FOR CO2 TRANSPORT PROPERTIES APPROXIMATION FUNCTIONS

| Coefficient | Absolute pressure | |
|---|---|---|
| | ***17.5MPa*** | ***20MPa*** |
| $A'_{\lambda_{CO_2}}$ | 8.94 | 10.11 |
| $B'_{\lambda_{CO_2}}$ | 0.0645 | 0.0637 |
| $A"_{\lambda_{CO_2}}$ | 1206 | 1284 |
| $B"_{\lambda_{CO_2}}$ | 3.34 | 3.24 |
| $A'_{\mu_{CO_2}}$ | 15.7 | 13.9 |
| $B'_{\mu_{CO_2}}$ | 0.0258 | 0.0285 |
| $A"_{\mu_{CO_2}}$ | 740 | 888 |
| $B"_{\mu_{CO_2}}$ | 5.01 | 4.2 |

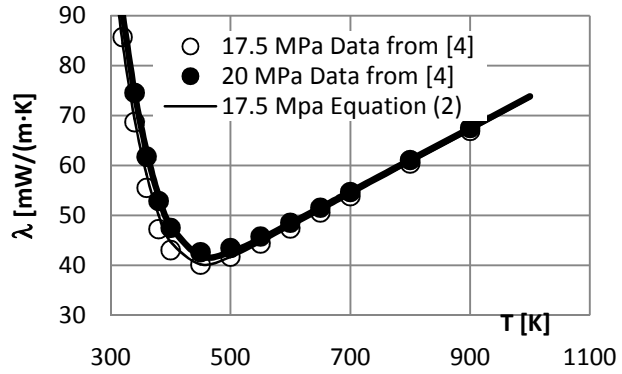


Fig. 3. Thermal conductivity of supercritical $CO_2$

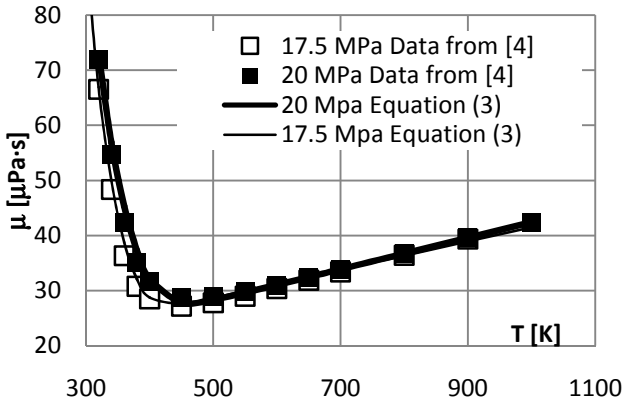


Fig. 4. Viscosity of supercritical $CO_2$

Figures 3, 4 show comparison of the data from [4] with the formulae (2) and (3) for transport properties of the supercritical $CO_2$

Helium was modeled as an ideal gas with the temperature dependent transport properties:

$$R_{He} = \frac{R}{m_{moleHe}} = \frac{8.3144621\ J/(mol \cdot K)}{0.0040026\ kg/mol}$$

$$c_p = 5193\ J/(kg \cdot K)$$

$$\lambda_{He} = 56 + 0.31 \cdot T[K] \quad mW/(m \cdot K)$$

$$\mu_{He} = 0.45 \cdot T[K]^{0.67}\ \mu Pa \cdot s$$

*C. Modeling of solid material properties*

The following properties are assumed for tungsten and F82H steel:

$$\rho_W = 19254\ kg/m^3$$

$$c_W = 138\ J/(kg \cdot K)$$

$$\lambda_W = 115 + 0.012 \cdot T[K] \quad W/(m \cdot K)$$

$$\rho_{\mathrm{F82H}} = 7854\ kg/m^3$$

$$c_{\mathrm{F82H}} = 470\ J/(kg \cdot K)$$

$$\lambda_{\mathrm{F82H}} = 33 \quad W/(m \cdot K)$$

Table II presents values of the Young modulus and thermal expansion coefficient for F82H steel used in structural analysis of the system. Linear interpolation between tabulated values was applied. Reference temperature of 22°C was used.

TABLE II. STRUCTURAL PROPERTIES FOR F82HSTEEL

| Temperature | Absolute pressure | |
|---|---|---|
| | *Young Modulus* | *Thermal Expansion* |
| 20°C | 216GPa | - |
| 22°C | - | $1.04 \cdot 10^{-5}\ 1/°C$ |
| 450°C | 193GPa | - |
| 700°C | 160GPa | $1.24 \cdot 10^{-5}\ 1/°C$ |

*D. Properties of liquid lithium carrying parts*

The parts carrying liquid lithium are assumed solid with properties of liquid lithium approximated from the data in [5]:

$$\rho_{Li} = 278.5 - 0.04657 \cdot \mathrm{T[K]} + 274.6 \left(1 - \frac{\mathrm{T[K]}}{3500}\right)^{0.467} \frac{kg}{m^3}$$

$$c_{Li} = 4754 - 0.925 \cdot \mathrm{T\ [K]} + 2.91 \cdot 10^{-4} \cdot \mathrm{T[K]}^2 \frac{J}{kg \cdot K}$$

$$\lambda_{Li} = 22.28 + 0.05 \cdot \mathrm{T[K]} - 1.243 \cdot 10^{-5} \cdot \mathrm{T[K]}^2 \quad \frac{W}{m \cdot K}$$

Evaporation of the liquid lithium on the front surface was modeled as approximation of the data from [6]:

$$q_{Li}^{evap} = \frac{145920 \cdot 10^{9.3984 + 0.036322 \cdot \mathrm{T[°C]} - 2.1251 \cdot 10^{-5} \cdot \mathrm{T[°C]}^2}}{6.02214 \cdot 10^{23}} \frac{W}{m^2} \qquad (4)$$

*E. Mesh Generation*

Mesh used for 2D analysis is presented on fig 5. Mapped mesh was used in fluid regions allowing detailed boundary layer discretization.

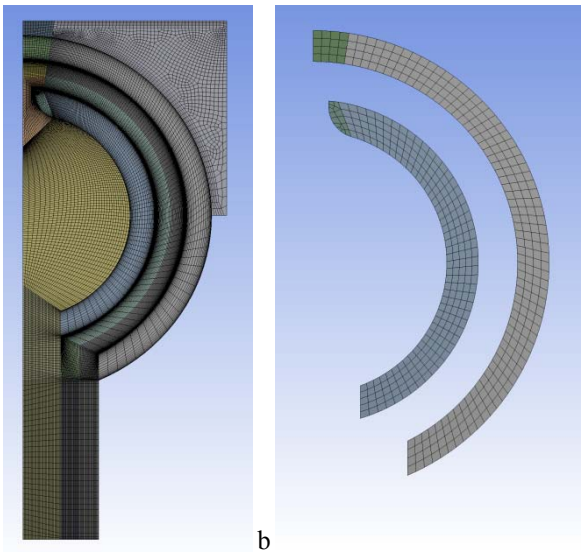


Fig. 5. Meshes used in 2D analysis: a) CFD and conjugated heat transfer b) structural analysis.

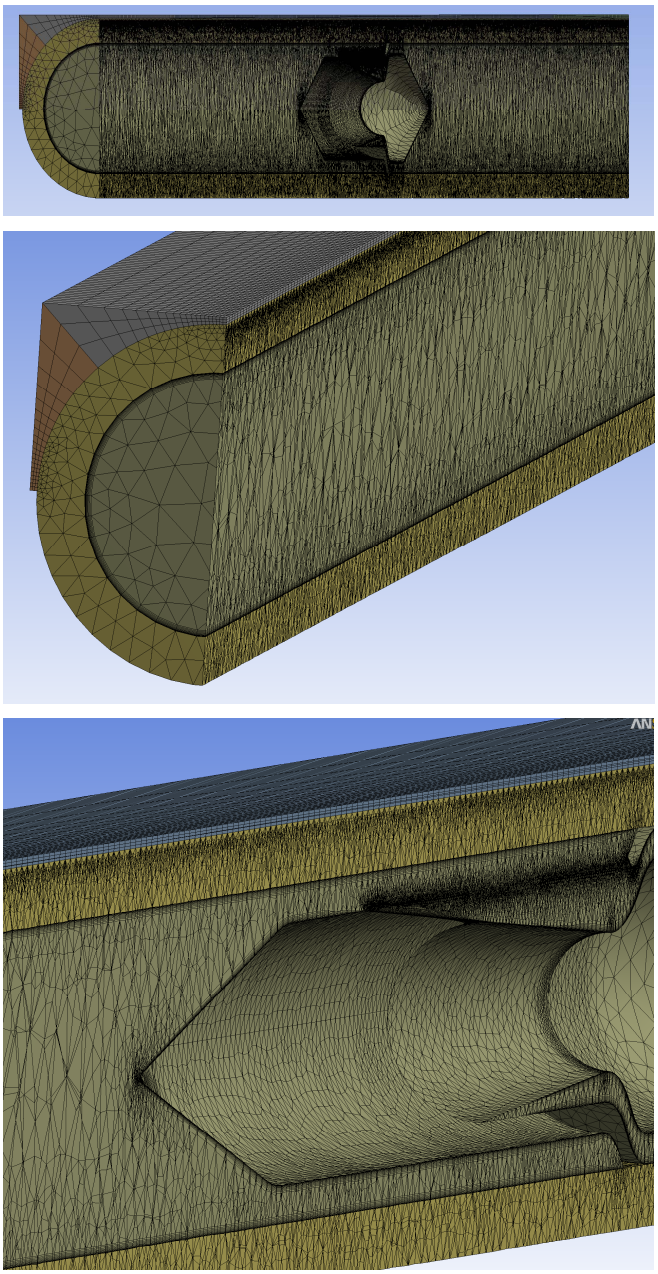

Fig. 6. Fragment of the mesh used in 3D CFD and conjugated heat transfer analysis

For 3D analysis automatic unstructured tetrahedral mesh was generated in the flow region, however boundary layers of prism elements were created on the fluid side of the fluid solid interface, as shown on fig. 6.

## III. Validation of the Model

Present model was validated using comparison with the numerical simulations of the T-tube flow with FLUENT code reported in [7]. This calculation used tungsten tubes and armor, and helium as a coolant. Geometrical and flow parameters and incident heat flux of 10MW/m$^2$ were used the same as in [7]. Fig. 7 shows very close behavior of both simulations in all regions except in the vicinity of impingement, where present model has finer mesh.

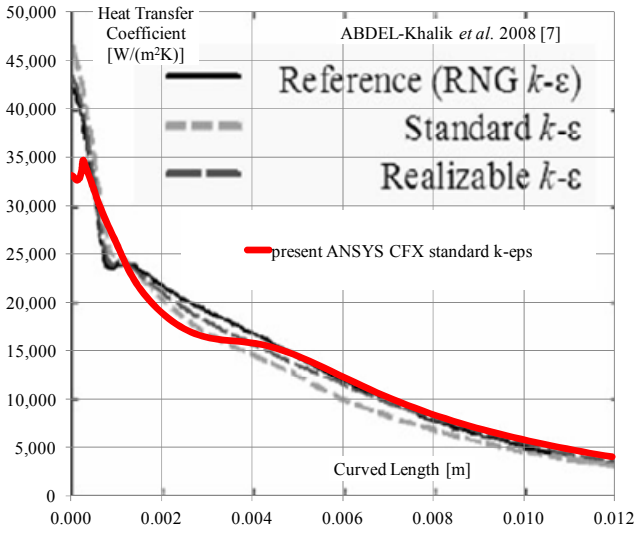


Fig. 7. Validation of the model using 2D numerical simulations of helium flow in T-tube

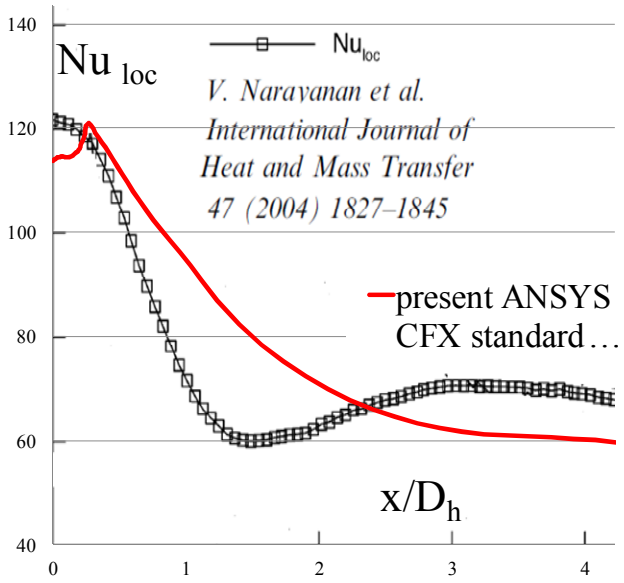


Fig. 8. Validation of the model using 2D confined impinging jet flow

To make sure that correct values of heat transfer coefficient were obtained in the calculations the model was validated against experimental results for confined jet impinging on a flat surface [8]. Numerical results with current model show similar distribution, and the same maximum and minimum values of local Nusselt number

## IV. 2D Simulations

Two dimensional simulations were performed to optimize the geometry of the cooling. Figure 9 presents results of the 2D comparative simulations using tungsten divertor components, with inlet temperature 185°C, inlet pressure 10MPa, and inlet velocity of 24m/s. Numerical simulations show that supercritical CO2 provides more efficient cooling of the front wall with the same initial parameters of the coolant.

Maximum temperature on the armor is 854°C for supercritical $CO_2$ compared to 1109°C for helium

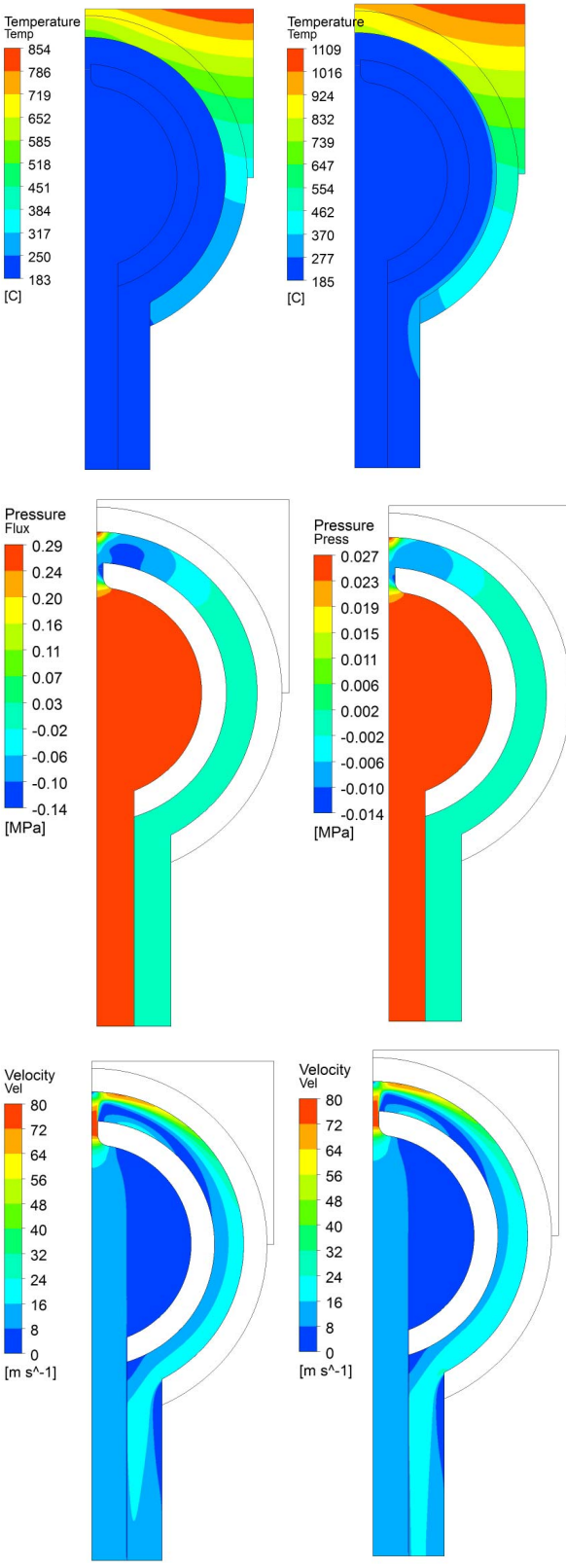


Supercritical $CO_2$ He

Fig. 9. 2D numerical simulation s using wit different coolants

## V. 3D SIMULATIONS

Three dimensional numerical simulations were performed using F82H tubes and liquid lithium armor. Variable incidental heat flux was imposed on the front wall:

$$q_{ext} = 2.1 + 10 \cdot e^{-|x[m]|/0.015} \frac{MW}{m^2}$$

This heat flux was corrected using lithium evaporative heat flux relation (4). Supercritical $CO_2$ with inlet temperature of 185°C was used.

Results for the symmetrical T-tube simulations presented on figures 10-12 show that efficient cooling of the front surface can be achieved, with the flow rate of 0.3 kg/s, leading to pressure drop of 1.34MPa, which results in the pumping power requirement of 1352W

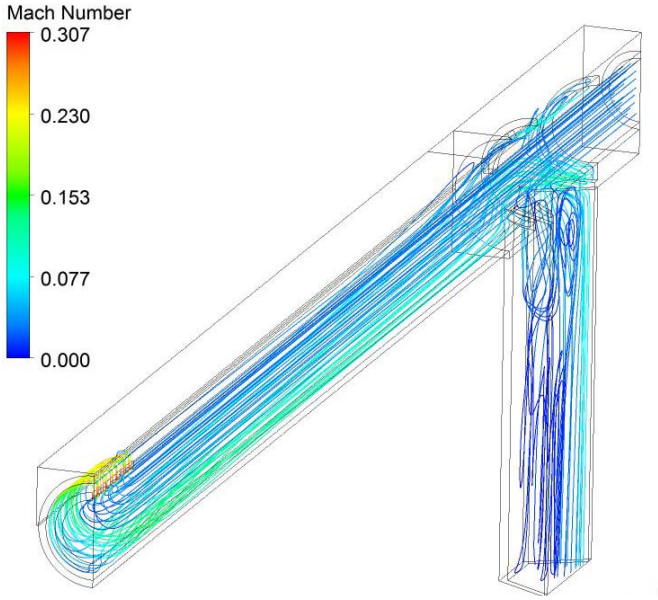


Fig. 10. 3D numerical simulations of the T tube cooling system. Stream lines colored by the values of the local Mach number

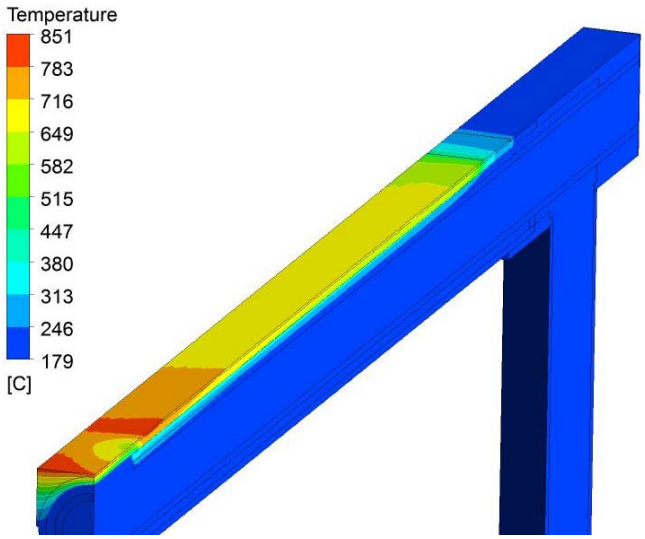


Fig. 11. 3D numerical simulations of the T tube cooling system. Temperature distribution

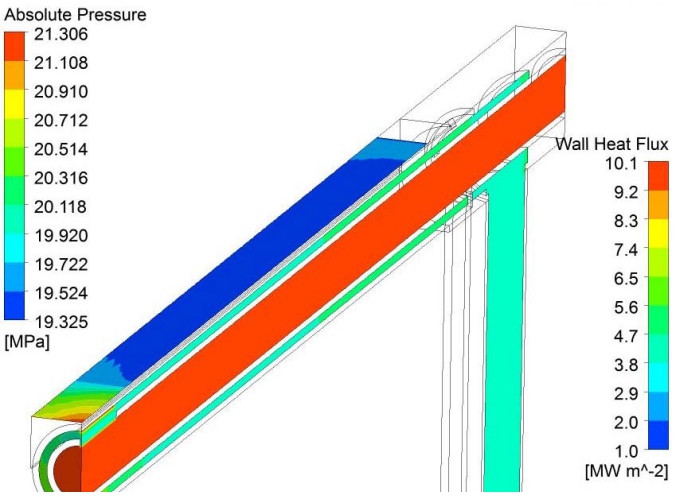


Fig. 12. 3D numerical simulations of the T tube cooling system. Coolant pressure distribution, and front wall heat flux distribution

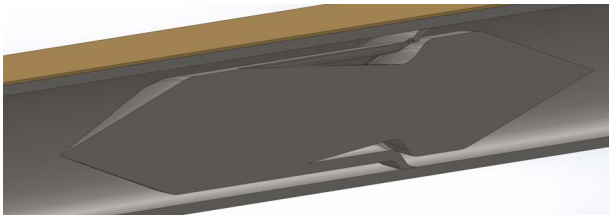

Fig. 13. Optimized T-tube type insert design

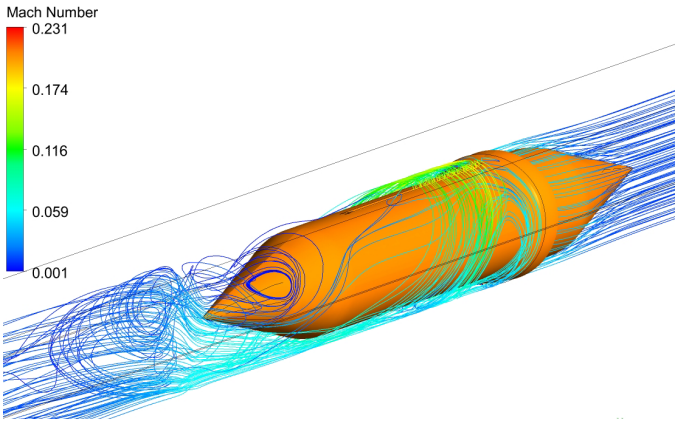


Fig. 14. 3D numerical simulations of the T tube cooling system. Stream lines colored by the values of the local Mach number

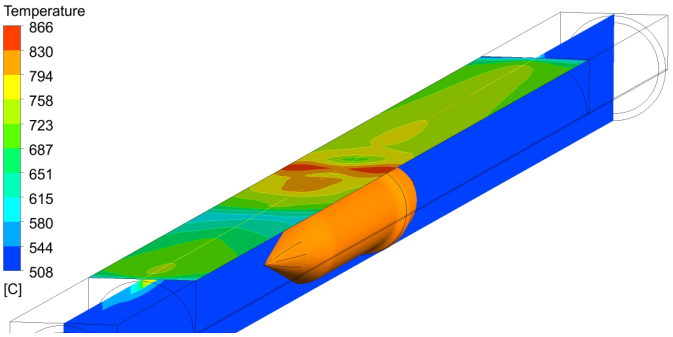


Fig. 15. 3D numerical simulations of the T tube cooling system. Temperature distribution

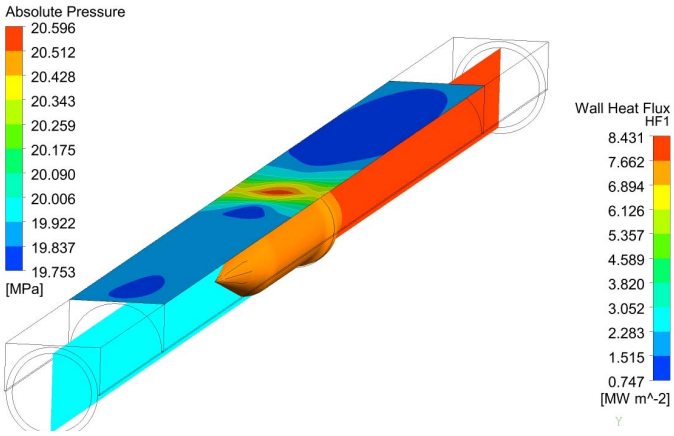


Fig. 16. 3D numerical simulations of the T tube cooling system. Coolant pressure distribution, and front wall heat flux distribution

Figure 13 show cross-section of the insert which allows creating an impinging jet situation similar to T-tube in the area of the maximum heat flux while maintaining main flow direction. Results for the optimized T-tube simulations presented on figures 14-16 show that efficient cooling of the front surface can be achieved, with the flow rate of 0.15 kg/s, leading to pressure drop of 0.59MPa, which results in the pumping power requirement of 317W.

## VI. CONCLUSIONS

Supercritical $CO_2$ can be used as an efficient coolant of the divertor cooling system.

Optimized T-tube configuration allows significant reduction of the pumping power at the comparative cooling rate

Further optimization of the cooling system is needed to reduce temperature on the front wall

## REFERENCES

[1] "ANSYS CFX-Solver Modeling Guide," ANSYS, Inc., November 2010.

[2] "Structural Analysis Guide," ANSYS, Inc., November 2009.

[3] R. Span, and W. Wagner, "A New Equation of State for Carbon Dioxide Covering the Fluid Region from the Triple-Point Temperature to 1100K at pressures up to 800 MPa," J. Phys. Chem. Ref. Data, vol. 25, No. 6, 1996, pp 1509-1596.

[4] V. Vesovic, W. A. Wakeham, G. A. Olchowy, J. V. Sengers, J. T. R. Watson, and J. Millat, "The transport Properties of Carbon Dioxide," J. Phys. Chem. Ref. Data, vol. 19, No. 3, 1990, pp 763-808.

[5] H. W. Davison, "Compilation of Thermophysical Properties of Liquid Lithium," NASA TN D-4650, July 1968.

[6] R.F. Mattas et al. "ALPS–advanced limiter-divertor plasma-facing systems" Fusion Engineering and Design 49–50, 2000, pp 127–134.

[7] S. I. Abdel-Khalik, "Thermal-Hydraulic Studies in Support of the Aries-CS T-Tube Divertor Design" Fusion Science and Technology, vol. 54, 2008, pp 864-877

[8] V. Narayanan, J. Seyed-Yagoobi, P. H. Page "An Experimental Study of Fluid Mechanics and Heat Transfer in an Impinging Slot Jet Flow" Int. J. of Heat and Mass Transfer, vol. 47, 2004, pp. 1827-1845.